Why do tornados and hailstorms rest on weekends?

Daniel Rosenfeld[1]* and Thomas L. Bell[2]

ABSTRACT

This study shows for the first time statistical evidence that when anthropogenic aerosols over the eastern USA during summertime are at their weekly mid-week peak, tornado and hailstorm activity there is also near its weekly maximum. The weekly cycle in summertime storm activity for 1995–2009 was found to be statistically significant and unlikely to be due to natural variability. It correlates well with previously observed weekly cycles of other measures of storm activity. The pattern of variability supports the hypothesis that air pollution aerosols invigorate deep convective clouds in a moist, unstable atmosphere, to the extent of inducing production of large hailstones and tornados. This is caused by the effect of aerosols on cloud-drop nucleation, making cloud drops smaller and hydrometeors larger. According to simulations the larger ice hydrometeors contribute to more hail. The reduced evaporation from the larger hydrometeors produces weaker cold pools. Simulations have shown that too cold and fast-expanding pools inhibit the formation of tornados. The statistical observations suggest that this might be the mechanism by which the weekly modulation in pollution aerosols is causing the weekly cycle in severe convective storms during summer over the eastern USA. Although we focus here on the role of aerosols, they are not a primary atmospheric driver of tornados and hailstorms, but rather modulate them in certain conditions.

[1] The Hebrew University of Jerusalem, Institute of Earth Sciences, Jerusalem 91904, Israel.
[2] NASA/GSFC, Climate and Radiation Branch, Greenbelt, MD 20771, USA.
*To whom correspondence should be addressed. E-mail: daniel.rosenfeld@huji.ac.il

1. Introduction

This study puts to a statistical test the hypothesis that air pollution increases the chance of severe convective storms. The motivation for posing this question is based on physical considerations that are described in Section 1.2 of the Introduction. These considerations have already been partially supported by the observations of a weekly cycle in rainfall, storm heights, and large-scale vertical winds, made by *Bell et al.* [2008]. We believe this hypothesis does two things: 1) it provides a framework for understanding the observations originally reported by *Bell et al.* [2008]; and 2) it has been a very successful tool for predicting weekly cycles in other meteorological quantities, some of which have been reported elsewhere (e.g., lightning activity [*Bell et al.,* 2009a]), and fractional cloud cover and cloud-top temperatures (mentioned in *Bell et al.,* 2009b), and some of which (weekly cycles in hailstorm and tornado activity) are reported here.

We believe that a strong observational case is made in this paper for the existence of a weekly cycle in hailstorm and tornado activity over the eastern U.S. during the summer. We would not have looked for such evidence had we not had the physical theory we present below to guide us. Nevertheless, we should emphasize that the observations we report here only show a correlation in hailstorm and tornado activity with the well-established weekly cycle in pollution over the same area, and correlations do not prove causality. These observations provide the impetus for more detailed observational studies and advances in modeling of the effects of aerosols on storm development that will be capable of establishing the causal connection, a connection we can only present as a hypothesis here.

47
48 1.1 The weekly cycle in rain intensity and lightning activity
49
50 The weekly cycle of working weekdays and resting weekends is associated with
51 weekly-varying levels of particulate air pollution [e.g., *Bell et al*., 2008]. This cycle has
52 been shown to be associated with weekly cycles of midweek rainfall amounts, storm
53 heights [*Bell et al*., 2008; *Bell et al*. 2009b], and lightning activity [*Bell et al*., 2009a] in
54 the warm and moist climate of summer months in the southeast USA. It was
55 hypothesized that this is caused by mid-week enhanced particulate air pollution
56 invigorating convective storms, as will be described in Section 1.2. Theoretical
57 considerations and cloud simulations, described in Section 1.3, support this hypothesis.
58
59 1.2 The physical basis for aerosols invigorating convective clouds
60
61 Particulate air pollution can invigorate convective storms whose cloud bases are
62 warm enough that the cloudy air has to rise several km before reaching the freezing level.
63 In clouds forming in pollution-free air, rain can develop and precipitate from the lower
64 parts of the cloud without freezing. This early rain can be inhibited by the pollution
65 aerosol particles that act as cloud-drop condensation nuclei (CCN) and nucleate greater
66 concentrations of smaller cloud drops that are slower to coalesce into rain drops [*Gunn*
67 *and Phillips*, 1957]. In clouds with warm cloud-base temperatures the freezing level is
68 several km above cloud base, so that rain can develop and fall from the rising air in the
69 cloud. Because the effect of aerosols is to suppress coalescence, rain is delayed and a
70 larger fraction of the cloud water ascends above the 0°C isotherm level, where it is
71 accreted on ice precipitation particles that fall and melt at lower levels [*Molinié and*
72 *Pontikis*, 1995; *Andreae et al*., 2004]. The additional release of latent heat of freezing

aloft and reabsorbed heat at lower levels by the melting ice implies greater upward heat transport for the same amount of surface precipitation in the more polluted atmosphere. In addition, greater evaporative cooling of the cloud water in the downdrafts increases further the vertical heat exchange [*Lee et al*., 2010]. This means that more instability is consumed for the same amount of rainfall. The inevitable outcome is invigoration of the convective clouds [*Rosenfeld et al*., 2008]. Cloud simulations have supported this hypothesis by showing that updrafts increase in warm-base clouds (~ 20°C) with added aerosols that suppress the warm-rain processes [*Khain et al*., 2004, 2005, 2008; *Khain and Lynn*, 2009; *Wang*, 2005; *Tao et al.,* 2007; *Li et al., 2008; Lee et al*., 2008a; *van den Heever et al*., 2006; *van den Heever and Cotton*, 2007; *Ntelekos et al*., 2009]. According to these simulations, invigoration was not necessarily associated with added rainfall amounts. Enhanced rainfall was simulated only in warm, moist, unstable and low shear environments [*Khain et al*., 2008; *Lee et al*., 2008b; *Fan et al.,* 2007 and 2009]. The stronger updrafts and downdrafts resulted in more coherent organization of the simulated convection that feeds back into the intensity of the storms [*Ntelekos et al*., 2009; *Lee et al*., 2010]. The invigoration was supported also by observations of more polluted convective clouds growing taller [*Koren et al*., 2005, 2008 and 2010] and invigorating the circulation systems (*Zhang et al*., 2007; *Bell et al*., 2008).

1.3 The physical basis for aerosols enhancing lightning, hail and tornadoes

The invigorated updrafts with added supercooled water and ice hydrometeors provide the conditions for enhanced cloud electrification [*Molinié and Pontikis*, 1995; *Williams et al*., 2002; *Andreae et al*., 2004]. However, the observational evidence was questioned due to the difficulty in separating the roles of thermodynamics and aerosols

98 [*Lyons et al*., 1998; *Williams and Stanfill*, 2002; *Williams et al*., 2002; *Williams*, 2005].
99 Critical supporting observational evidence for the validity of the invigoration hypothesis
100 was obtained very recently, where volcanic aerosols, whose variability was completely
101 independent of meteorology, were observed to invigorate deep convective clouds over the
102 northwest subtropical Pacific Ocean and more than double the lightning activity [*Yuan et*
103 *al*., 2011; *Langenberg*, 2011].
104 The greater amount of supercooled cloud water in polluted situations means greater
105 growth rate of ice hydrometeors. The stronger updrafts mean that larger hail stones can
106 be suspended in the cloud before falling to the ground. Therefore, it is reasonable to
107 expect that clouds in more polluted air would produce larger hail stones. This is
108 supported by some observations [*Andreae et al*., 2004; *Wang et al*., 2009] and
109 simulations [*Storer et al*., 2010; *Khain et al*., 2011].
110
111 The dynamics of convective storms respond to the initial changes in precipitation by
112 changes in the downdrafts and their evaporative cooling, which feed the cold pools and
113 their gust fronts. Early simulations [*Gilmore et al*., 2004; *van den Heever and Cotton,*
114 2004] showed that storm dynamics are very sensitive to changes in hydrometeor size,
115 such that smaller hydrometeors create larger cold pools and stronger gust fronts that feed
116 back to the storm dynamics. Colder downdrafts would produce a faster moving gust front
117 that would tend to cause faster propagation of the squall line. A supercell can be regarded
118 as a quasi-steady-state convective storm, where the gust front is not outrunning and
119 undercutting the updraft in the feeder clouds. Less evaporative cooling into the downdraft
120 would reduce the cooling and extent of the cold pool. A slower moving gust front with

121 respect to its originating cell would drive the convective system closer to a state of a
122 supercell, which is the typical cloud type that produces large hail and tornadoes.
123 Supercell storms inherently form in a high wind shear environment. The wind shear
124 causes the main rain shaft with the associated downdraft to be displaced from the low
125 level updraft. This is the mechanism that allows the longevity of the supercell storms, and
126 hence increases their vigor and potential for generating tornados and large hail. The
127 simulations of Fan et al. (2009) showed that aerosol-induced invigoration of the updraft
128 aloft requires a weak wind-shear environment. With little aerosol-induced invigoration
129 expected during the strong-wind-shear conditions that are favorable for large hail and
130 tornadic storms, the mechanism in question by which aerosols increase the chance of
131 tornados, cannot be fully explained by the convective invigoration hypothesis (Rosenfeld
132 et al., 2008). Here we propose that the aerosol-induced changes in the precipitation
133 particle-size distribution reduce the evaporative cooling in the precipitation shaft. The
134 way by which it might enhance tornadogenesis is described next.
135 *Ludlam* [1963] proposed that air parcels within the downdraft tend to be less
136 negatively buoyant (warmer) in tornadic vs. nontornadic supercells. Tornadic vortices
137 increase in intensity and longevity as downdraft parcel buoyancy increases, because
138 colder parcels are more resistant to lifting. This was supported by observational and
139 numerical modeling studies [*Markowski et al*., 2002 and 2003]. Simulations of the
140 sensitivity of tornadogenesis to the hydrometeor size distribution, done at the high
141 resolution of 100 m [*Snook and Xue*, 2008], showed that by merely increasing the
142 hydrometeor size an EF2 intensity tornado was produced by the model. When the cold
143 pool is strengthened by decreasing the hydrometeor sizes, the updraft is tilted rearward by

144 the strong, surging gust front, causing a disconnection between low-level circulation
145 centers near the gust front and the mid-level mesocyclone.
146 Clouds with smaller drops were observed to produce larger rain drops for the same
147 rain intensity [*Rosenfeld and Ulbrich*, 2003]. This was confirmed by simulations of warm
148 rain [*Altaratz et al*., 2008] and mixed phase clouds [*Khain et al*., 2011]. Incorporating
149 this effect in simulations of an idealized supercell thunderstorm [*Lerach et al*., 2008]
150 showed that the added aerosols suppressed the precipitation and produced larger and
151 fewer hailstones and raindrops. This produced an EF-1 tornado. The unpolluted
152 simulation produced more precipitation evaporative cooling, and thus a stronger surface
153 cold pool that surged and destroyed the rear flank downdraft structure. This resulted in a
154 single gust front that propagated more rapidly away from the storm system, separating the
155 low-level vorticity source from the parent storm and thus hindering the tornadogenesis.
156 Rosenfeld and Ulbrich [2003] attributed the aerosol effect on precipitation particle
157 size distribution to the larger number of raindrop embryos that form in warm rain
158 processes as compared to precipitation initiation by ice precipitation embryos in mixed
159 phase clouds. For the same aerosol concentrations, warmer cloud base means larger
160 distance to the freezing level, where cloud drops can grow bigger and coalesce faster into
161 rain drops. Therefore, this aerosol effect on the precipitation particle size distribution and
162 in turn on tornadogenesis is expected to be more pronounced for clouds with warmer
163 bases. According to Figure 1, sufficiently warm cloud base for the aerosol effects (>
164 ~15°C) occur during the months June-August over the eastern part of the USA, to the east
165 of longitude 100W. During the summer months this line lies along the dew point
166 isotherm of 15°C within a sharp gradient of increasing dew points eastward. The analysis

of the aerosol effects in this study is focused at these times and places. Interestingly, the strongest hailstorms occur just to the west of 100W. Williams et al. (2005) ascribed this to the fact that cloud-base height is sufficiently high and cold while the instability is still very high, such that warm rain is prevented from forming in the short distance between cloud base and the freezing level regardless of the aerosol amounts, allowing large accumulations of supercooled water that feed the growth of large hail. The cloud base is still not too cold to deplete the amount of potential condensates and supercooled water that are required for the growth of large hail. The cloud base west of 100W is thus too cool for aerosols to be a major factor in modulating the hailstorms.

In this brief review we have shown that there is a physical basis for the hypothesis that added aerosols can contribute to the occurrence of large hail and tornadoes. In the next sections the hypothesis that the weekly cycle in pollution aerosols is associated with a similar cycle in the hail and tornadoes will be tested using observational data for hail and tornado activity.

2. The data

Based on the physical considerations above, we expect that the occurrences of severe convective storms would be enhanced in a more polluted atmosphere during the summer months in the eastern USA, where the convective storms form in a warm and moist atmosphere and are least forced by synoptic weather systems such as cold fronts. In order to test whether there is a weekly cycle, daily counts of tornados or hail, categorized by intensity, were analyzed.

Data for tornado and hail observations in the U.S.A. were obtained from the web site of the Storm Prediction Center (SPC) of the National Oceanic and Atmospheric

192 Administration [*SPC Data*, 2010]. The observational data maintained by the SPC are
193 based on reports collected by local National Weather Service Forecast Offices from a
194 wide variety of sources (trained spotters, emergency personnel, the media, the general
195 public, etc.). The assignment of tornado strength on the enhanced Fujita scale [*EF*] for a
196 tornado probably reflects both estimates of the intrinsic strength of the tornado and
197 valuations of the level of property damage found along the path of the tornado (see, for
198 example, *Doswell and Burgess* [1988]). A characteristic largest hailstone size is assigned
199 to hailstorm events, according to the NOAA National Weather Service (2007) Storm
200 Data Preparation rules. Hail diameters are given in inches. One inch equals 2.54 cm.
201 The NOAA Warning Coordination Meteorologist attempts to identify and remove
202 duplicate observations and to link storms that span several jurisdictions. The data we
203 used were current as of 16 March 2010.
204
205 *Schaeffer and Edwards* [1999] suggest a number of possible biases in these data:
206 tornados generally go unreported where no one lives; both population and population
207 awareness has increased over the years; and the adoption of warning systems has made
208 people more alert to tornados. More tornados are observed near populated areas than
209 away from them. Storms that are particularly severe are probably missed less often,
210 however. The total numbers of tornados and of hailstorms have generally trended
211 upwards with the years (Figure 2). The conventions for attributing a given Fujita scale to
212 a storm have also evolved (e.g., Schaefer and Edwards, 1999). Rapid increases in the
213 numbers reported may be due to the introduction of new technology: implementation of
214 the WSR-88D radars with Doppler capability in about 1991, for example, may have led
215 to increased reporting of tornados after that date. An analysis by *Ray et al*. [2003]

suggests that tornados are reported more often near population centers and that tornado occurrences prior to 1992 may have been underestimated by about 40%.

The observational biases that may be present in the data can easily be imagined to change with the day of the week. Weekly changes in media coverage are possible, for instance. Despite these possibilities, we report later in the paper that we see no signs of a weekly cycle in the less populated western half of the U.S. and no signs of a cycle during the spring season in the eastern half. It is not easy to think of a plausible sociological bias that is present in the eastern half of the country but absent in the western half, or one that is absent in the spring and then appears in the summer. We also find that the weekly cycle in tornado and hail activity seen in the eastern half of the U.S. agrees well with the weekly cycle seen in other indicators of severe storm activity such as lightning and extent of vertical development of the storm clouds (indicators that are not subject to the same concerns about weekly biases in the observational system). These same indicators show no significant weekly cycle in the western half of the U.S. (Bell et al., 2008; 2009a and 2009b). This suggests that whatever physical mechanisms are modulating severe storm activity in the east during the summer are also affecting tornado and hail activity. The evidence we report here strongly suggests, we believe, that the weekly cycles in tornado and hail activity are real. Attempts to explain them as simply the result of weekly shifts in coverage by the observational network require constructing a rather tortuous and contrived picture of societal behavior.

In preparing the data for analysis, we edited a small fraction of the data entries based on the recommendations accompanying the data provided by the SPC and on the need to resolve various ambiguities. Entries with missing state identifications were ignored.

Entries with either zero latitude or longitude locations were ignored. Entries with negative Fujita scales were ignored (25 cases encountered). Apparently misidentified time zones were corrected. Multiple entries associated with a single tornado event were consolidated into one entry (not an issue in the hail dataset). Tornados that crossed state boundaries were treated as two separate events, however. Fifteen entries of hail sizes of 0.25 and 0.5 inches in 2007 were pooled with the entries for 0.75 inches. In total, fewer than 2% of the tornado dataset entries required editing. A far smaller percentage of hail data entries required editing. The number of tornado events for 1980–2009 in our edited dataset was approximately 33,000, while the number of hail events was approximately 235,000.

3. The data analysis

In the following subsections we provide details about the assumptions and methods used in the statistical analysis of the tornado and hailstorm data.

3.1. Statistical model of data under the null hypothesis

Testing the data for the presence of a weekly cycle requires a description of the statistics of the data under the null hypothesis, which is that the frequency of tornados or hailstorms does not vary cyclically with the day of the week. In modeling the statistics of hailstorms and tornado occurrences under the null hypothesis, we try to accommodate the known variations in statistics with the season and year. Our goal is not to determine the "true" seasonal cycle or decadal trend but simply to produce something likely to be closer to the truth than ignoring the seasonal cycle or year-by-year trend altogether.

We used the average seasonal cycle over the years 1980–2009 to represent the modulation of the expected count with the seasons (i.e., with the day of the year). Though we used 15 years of data (1980–1994) prior to the period we are concentrating on (1995–2009), they were used only to help establish the background seasonal cycles and decadal-scale trends, and for the bootstrap statistical analysis described later. The seasonal cycle estimated from 30 years of data is smoother than the cycle estimated using 15 years (1995–2009), as would be expected, but is not substantially different. We believe that using data prior to 1995–2009 to increase the stability of our estimate of the seasonal cycle increases the overall robustness of our statistics, but that if we had confined our averaging to the years 1995–2009 our conclusions would not be changed in any substantial way.

We show in Figure 3 the average number of tornados reported east of longitude 100W for each day of the year. The averages for each day of the year in Figure 3, though based on 30 years of data, exhibit quite a lot of variability from day to day, almost certainly due to the sample size (30 samples, one for each year) in the daily averages. Note that averages for each day of the year include data from all days of the week (Sun through Sat). Rather than trying to build a smoother, parameterized model for the seasonal cycle, we applied a kind of running average to the 365 daily averages (leap years treated as having 365 days). The filter devised by *Lee* [1986] produced a satisfactory curve when we applied the filter twice with a window size of 11 days (on either side of the central value), as shown in Figure 3. The Lee filter produces a smooth fit to the data but tries also to capture sudden jumps in the local mean. The climatological average

287 compares well to the average obtained by *Brooks et al*. [2003], though *Brooks et al*.
288 [2003] report averages for a different region and time period.

289 The annual counts for each year from 1980 to 2009 vary quite a bit from year to year
290 (e.g., see Figure 2), possibly attributable to large-scale influences such as ENSO or to the
291 unpredictable fluctuations in weather, but there appears to be a decadal trend in the
292 counts as well. Some of these trends might be explained by societal changes, such as
293 increasing awareness of the danger of tornados, and in the methods of collecting the data,
294 as discussed by *Schaefer and Edwards* [1999].

295 We found that the seasonal cycles of the different tornado strengths are fairly similar
296 (although the small numbers of high-EF tornados make comparisons of averages
297 difficult), when the seasonal cycle of counts for a particular EF values is normalized by
298 the total number of storms at that EF value. The seasonal cycles for different hail sizes
299 are very similar. We should note, however, that the similarity in the seasonal cycles is
300 used very little in the analyses presented here.

301 In order to test whether the tornado/hailstorm statistics differ significantly from what
302 would be expected under the null hypothesis that there is no weekly cycle, we need a
303 statistical model for the expected number of storms under the null hypothesis. Since we
304 only test data from portions of a year rather than for full years, we require a model that
305 describes the variation in the expected number of storms as a function of the day of the
306 year. We assume that the expected number of tornado/hail events for a given day and
307 season/year is proportional to the total number of storms for that season (thus capturing
308 the interannual variability in Figure 2) and to the average number of storms for the given
309 day of the year (as represented by the smooth curve in Figure 3). If there is a weekly

cycle, we generally assume in our analyses that the cycle is described as a sinusoidal oscillation modulating the expected number given by our null-hypothesis model [this is made precise by Equations (2) and (3) below]. Another possible shape for the weekly modulation, a step function, is investigated later.

To represent the expected number of tornados $n_0(y,j)$ in year y and day j for summertime tornados (June 1 – August 31, i.e., $152 \le j \le 243$) under the null hypothesis, then, we assume that the number is proportional to the number of tornados that summer $n(y)$ and to the seasonal cycle $f(j)$ represented by the smooth curve in Figure 3. Thus,

$$n_0(y,j) = n(y)\frac{f(j)}{\sum_{j'=152}^{243} f(j')}. \quad (1)$$

If $n(y,j)$ is the actual number of observed storm occurrences in year y for day j, $j = 1,\ldots,$ 365 (or 366 in a leap year), we define the ratio variable

$$r(y,j) = n(y,j)/n_0(y,j), \quad (2)$$

which has an average very near 1 when averaged over all years of data, or when averaged over all j, by construction. (Hailstorm statistics are similarly treated, using the climatology of hail based on the years 1980–2009.)

3.2. Statistical model of weekly cycle

We determine whether there is a weekly cycle in the ratio variable $r(y,j)$ by fitting the time-dependent data $r(t)$ to a 7-day sinusoid

$$r(t) = r_0 + r_7 \cos[\omega_7 (t - \varphi_7)] + \varepsilon(t) \quad (3)$$

with $\omega_7 = 2\pi/(7 \text{ days})$, where r_0 is the mean of the ratio variable, r_7 is the amplitude of the cycle, and φ_7 is the time during the week when the weekly cycle peaks. The error in the

fit is denoted by $\varepsilon(t)$. The time t is measured in days starting from an arbitrary date (we used $t = 0$ on Tuesday, 1 January 1980).

Statistical tests for the fit depend to some extent on an implicit assumption that the statistics of $r(t)$ don't change with the year or month. Although this is difficult to check with a short time series, we have tried to do this using some tests that seem likely to expose such a variation if it exists. We examined the variance of $r(t)$ calculated from the daily values of $r(t)$ over the 92 days of a single season, and plotted the variance versus the number of observed tornados for that season, and did not see signs of a change in the variance from those summers with relatively few tornados compared with those with many. We also examined the variance of $r(y,j)$ for each Julian day j, $j = 1,\ldots,365$, over the thirty years of data $y = 1980–2009$. When the variance is plotted versus the mean tornado count for a given day j, denoted above by $f(j)$, we find that the variance declines with the tornado count approximately as $f(j)^{-0.62}$. Since $f(j)$ itself only varies by approximately a factor of 3, this suggests that the variance of $r(t)$ ranges only over about a factor of 2 in size. Although we could adjust our statistical analysis to try to accommodate this possible variation, it would be at the cost of considerably more complexity in the analysis and very little gain in knowledge. The bootstrap analysis method described later also tends to circumvent the assumption of homogeneity of the statistics of $r(t)$, though not entirely.

It is perhaps worth reminding the reader here that by fitting the data to a pure sinusoid (Equation 3) we are not assuming that this is in fact an exact description of the weekly cycle in the data. A periodic signal with period 7 days can always be expressed as a sum of sinusoids with periods of 7 days and their higher harmonics. The higher

357 harmonics tend to be noisier and harder to estimate from small amounts of data, and we
358 have chosen not to examine them. Because the sinusoid is fit using data from all days of
359 the week, the sinusoid makes better use of the data (generating more robust statistics)
360 than a search for a weekly cycle that uses only averages of data from single days of the
361 week, a practice that is fairly common in searches for weekly cycles in data. It is easy to
362 obtain averages for each day of the week and to estimate the uncertainty in the averages
363 using standard statistical techniques. (An example is shown in Figure 4, to be discussed
364 later.) However, unless one has an *a priori* hypothesis about which days of the week are
365 likely to be anomalously high or low, the investigator must first examine the averages for
366 each day of the week, and then decide which averages are representative of the weekly
367 high and low values of a putative weekly cycle, and finally carry out an *a posteriori*
368 statistical test to see if the difference of the selected pair of averages is "statistically
369 significant." In effect one has examined 21 pairs of averages and chosen the pair most
370 likely to have a statistically significant difference. Carrying out such an *a posteriori* test
371 is not completely straightforward, since the prior examination of 21 pairs of (probably
372 correlated) averages must be included in the estimation of the statistical significance of
373 the largest difference. This type of approach generally has lower statistical power in
374 detecting a weekly cycle than the test for a sinusoidal variation in the averages, which
375 entails testing only a single parameter, the amplitude r_7 of the cycle, to ascertain whether
376 there is an anomalous cycle. Hasselmann [1979] provides a thorough discussion of why
377 multi-variable testing for anomalous averages has less statistical power than testing a
378 single weighted average over all variables. See also the discussion of multi-hypothesis
379 testing by *Wilks* [2006].

A still more powerful test for a weekly cycle might be done if the precise shape of the weekly cycle can be guessed. For instance, one might imagine that the weekly cycle consists in a constant daily average for the weekend (Sat–Sun) and another constant average for the weekdays (Mon–Fri) (i.e., a step-function response), though it is far from obvious that such a response is likely to be an accurate description. We have tried such a test, and the statistical significance of such a postulated cycle is similar in size to the significance we calculate for a sinusoidal weekly cycle (these results are reported later, in Section 4.1).

3.3 Statistical tests for weekly cycle

We write $r_7 \cos[\omega_7(t - \varphi_7)] = c_7 \cos(\omega_7 t) + s_7 \sin(\omega_7 t)$ and use linear-least-squares fits to this expanded version of Eq. (3) for each of the n weeks of data to obtain the coefficients $c_7(i)$ and $s_7(i)$ for each week i of data, $i = 1,\ldots,n$. Each summer contains 13 weeks of data; for the 15 summers in 1995–2009, there are $n = 15 \times 13 = 195$ weeks of data. The variance of the coefficients $c_7(i)$ and $s_7(i)$ from week to week over the n weeks can be used to estimate the overall uncertainty σ_7 in the amplitude r_7, using $\sigma_7^2 = (\text{variance}[c_7(i)] + \text{variance}[s_7(i)])/n$, where we assume that the correlation of the coefficients from week to week is negligible and the number of samples (n weeks) for variance estimates is large enough that the coefficients c_7 and s_7 are approximately normally distributed. (We tested the time correlations of the fitted amplitudes from week to week and found the correlations to be statistically consistent with the assumed correlation 0.) As explained in more detail by *Bell et al*. (2008), the ratio $(r_7/\sigma_7)^2$ has a Fisher F distribution [e.g., *Fraser,* 1958, p. 202] with two degrees of freedom in the numerator and (2n–2) degrees of freedom in the denominator. The quantity r_7/σ_7 is a measure of the signal strength

405 (signal-to-noise ratio). The significance level p of the amplitude r_7, under the null
406 hypothesis that there is no weekly cycle, can be fairly accurately estimated from this ratio
407 as

408 $$p = \exp[-(r_7 / \sigma_7)^2], \quad (4)$$
409
410 as explained in much more detail by *Bell et al*. (2008). The estimate (4) gives nearly the
411 same result as the more complex Fisher F distribution. Note that this means that the
412 probability that r_7 is larger than 1.73 σ_7 is $p = 0.05$; in other words, for tests of the
413 significance of r_7 the threshold for significance is 1.73 σ_7 instead of the familiar "two-
414 sigma" estimate 1.96 σ_7 that the traditional normal distribution would suggest.

415 Note that the coefficient r_7 in Equation (3) is obtained by fitting all of the data,
416 following the same procedure described above that was used for each week of data, and is
417 related to the best-fit coefficients c_7 and s_7 by the formula $r_7^2 = c_7^2 + s_7^2$. The phase φ_7 is
418 obtained from $[7/(2\pi)] \tan^{-1}(s_7/ c_7)$ measured in days. Since $t = 0$ is a Tuesday in our
419 scheme, the phase φ_7 is measured relative to a Tuesday.

420 Because of the normalization of the observed number *n(y,j)* by the expected number
421 $n_0(y,j)$ in Eq. (2), the value of r_0 in (3) obtained by the fitting procedure is typically very
422 close to 1. [It is not exactly 1 because the seasonal cycle *f(j)* is based on an average over
423 all years (1980–2009) whereas our fits generally use only the years 1995–2009.]

424 The statistical significance of the amplitude r_7 is estimated both by the method
425 described above and by a second method. The second method of estimating the statistical
426 significance of the fitted amplitude r_7 uses a bootstrap approach in which the original data
427 are re-sampled in segments 11-days long in a way that destroys any 7-day periodicity in
428 the original data. Segment sizes of 11 days are used based on the belief that the

correlation of weekly-cycle fits to the segments from one segment to the next is small. Where we have checked, it is indeed small. For example, the week-to-week lagged correlations of the coefficients $c_7(i)$ and $s_7(i)$ calculated using the tornado data (east of 100W) for the 30 summers of 1980–2009 are found to be Corr[c_7, c_7] = 0.046, Corr[s_7, s_7] = – 0.114, and Corr[c_7, s_7] = – 0.0077; for the hail data they are Corr[c_7, c_7] = 0.032, Corr[s_7, s_7] = – 0.014, and Corr[c_7, s_7] = – 0.0051. Since there are about 390 weeks of data for this period, the 5% (2-sigma) significance threshold level for correlations is approximately $2/\sqrt{390} = 0.10$. Only one of the six correlations passes this threshold, barely. The hypothesis that the week-to-week correlations of the fits are zero can therefore not be rejected.

To randomize with respect to the day of the week, segments are selected that are displaced from the original segment anywhere from 7 days before to 6 days after the original segment (i.e., whose starting point is chosen from within a 14-day window). We choose segments from prior or future seasons up to 5 years away, instead of confining ourselves to data from the same year, to increase the number of replacement choices. Thus, for example, if the segment we are replacing starts on 10 August 2001, we may randomly select a segment from the original dataset beginning anywhere from August 3 to August 16 and from any year from 1996 to 2006. This tends to generate simulated datasets with statistics that change with the day of the year in the same way as the original dataset, as far as preserving the seasonality of the statistics and decadal trends, but having no real weekly cycles. Note that because we have access to years prior to 1995, we may select random segments from years as early as 1990 when a segment from year 1995 is being replaced. Note that because the statistics of the ratio variable *r(y,j)*

seem to be fairly constant from year to year (as discussed at the end of Section 3.2), we create simulated datasets starting with the original dataset for *r(y,j)* rather than of *n(y,j)* itself, thereby minimizing the impact of seasonal and interannual variability on the statistics of the simulated datasets.

Synthesized datasets assembled from the 11-day segments are used to estimate values of r_7 for each dataset, and the statistical significance of the value of r_7 obtained from the original dataset is set at the fraction of synthesized datasets with r_7 larger than that of the original value. We found that the two methods produced comparable significance levels p (the probability that the value of r_7 could equal or exceed its value under the null hypothesis $r_7 = 0$).

4. Analysis Results

4.1. Results for tornados east of 100W

In accordance with the hypothesis that the impact of air pollution on invigorating severe storms would be greatest in a moist and warm atmosphere, we follow our previous geographic partitioning [*Bell et al*., 2008 and 2009a], and examine data for the summer months, June–August, and areas east of 100W for all latitudes within the USA (our earlier studies were constrained by the latitudinal coverage of the satellite data we used). The longitude of 100W separates the moist air mass to the east, where invigoration can be expected, from the dry air masses to the west, where cloud bases are too high and cold to be substantially invigorated by added aerosols. This is evident in the map of climatological mean dew point temperature for July, shown in Figure 1a.

Hail and tornado data are available from 1950, but their quality has evolved over time. The completeness of the coverage has been improving, especially, we assume, for

476 the weaker and thus less noticeable events. Based on the evidence in Figure 2, overall
477 observational coverage of tornados seems to have stabilized since the mid 1990's,
478 whereas coverage of hail appears to have grown continuously. We have focused our
479 search on the period 1995-2009. This choice is also motivated by the results of Bell et al.
480 *[2008]*, where clear signs were reported of a weekly cycle in satellite estimates of
481 rainfall, in rain-gauge data, and in the induced modulation of the regional circulation
482 patterns for the period 1998–2005, and where evidence that the weekly cycle seemed to
483 weaken in earlier decades was found.
484 A weekly cycle in the aerosol impacts on storms depends on the existence of a
485 weekly cycle in anthropogenic aerosols. Ideally one would examine long-term records of
486 the concentration of cloud-condensation nuclei (CCN) near cloud base in order to
487 establish the existence of weekly cycles in the aerosols that directly influence storm
488 evolution. Continuous monitoring of CCN concentrations over the geographical scales of
489 interest is not yet available, unfortunately. As an indicator of anthropogenic emission of
490 aerosols, however, we have examined Environmental Protection Agency (EPA) datasets
491 for surface-level concentrations of particulate matter with particle diameters greater than
492 either 10 μm or 2.5 μm, respectively. These data were recently analyzed by *Bell et al*.
493 [2008]. A weekly cycle in both PM10 and PM2.5 is clearly to be seen in Figure 4. The
494 figure shows the fractional anomalies (deviations from the mean divided by the site
495 mean) observed at each site, averaged over all EPA sites. The weekly cycles of hail and
496 tornadic storms for the years 1995-2009, also shown in Figures 4 and 5, behave very
497 similarly to the cycle in the aerosols, with a distinct minimum on weekends.

When fits to the weekly cycle shown in Figure 4 using sinusoids are tested for statistical significance, the *p*-values (probability of the truth of the null hypothesis that there is no weekly cycle) are small, especially for hailstorms (of which there are many more events than for tornados). As mentioned above (see Section 3.2), one can carry out statistical tests for other functional shapes of the weekly-cycle response. When we fit the data to a step function with one constant during the weekend and another during the work week, we found the statistical significance (*p*-values) of such a response shape to be similar to what we found for the sinusoid, even though the sinusoid includes an extra parameter, the phase of the cycle. We found that a step function fits the tornado data with a $p = 0.013$ using a Student *t*-test and $p = 0.015$ from bootstrap estimation. A step function fits the hail data with a $p = 0.003$ using a Student *t*-test and $p = 0.0001$ from bootstrap estimation. (When *p* values get this low, estimates of *p* values can be very noisy.) Both of these step-function fits used data from 1995–2009, JJA, for the area east of 100W. Figure 6 shows plots of the weekly cycles and fits. (The constant portions of the step-function fits are not perfectly flat because of the effect of converting $r(t)$ to $n(t)$ using Equation 2, since it is $r(t)$ that is fit to the step-function but it is averages of $n(t)$ that are plotted in the figure.)

The temporal and spatial distribution of the weekly cycle matches the distribution of the warm, moist and unstable conditions in which aerosols have the strongest tendency to invigorate deep convective clouds [*Rosenfeld et al*., 2008]. During summer, the longitude of 100W coincides with the transition from the moist climate to the east of it to the hot and dry climate to the west, as shown in Figure 1a.

520 The moisture peaks in the months of June, July and August and reaches the northeast
521 USA, but starts to retreat southward during late August and September. The aerosol
522 invigoration effect on convective clouds can become apparent in moist atmospheres when
523 synoptic forcing is less dominant. In cool base clouds (i.e, temperature of about 10°C or
524 less) the effect diminishes [*Rosenfeld et al*., 2008]. This is in agreement with the spatial
525 and temporal distribution of the weekly cycle, as depicted in Figure 7. The figure shows
526 the state of the weekly cycle over three latitudinal bands east of 100W as a function of
527 the time of year. Each arrow represents the statistics for a 2-month period from the years
528 1995–2009. The length of the arrow shows the amplitude of the weekly cycle r_7 as a
529 fraction of the mean r_0. The direction indicates the day of the week when the sinusoidal
530 fit peaks. The color indicates the significance level p of the fit, reflecting the signal-to-
531 noise ratio of the fit. The figure shows that the transition from the synoptically forced
532 storms in the spring, when moisture levels are also much lower (Figure 1b), to the more
533 locally unstable storms that form in a moist unstable air mass in the summer is
534 accompanied by an increase in the weekly cycle modulation tending to have a mid-week
535 maximum. The return of the synoptic forcing and drier air in the early fall to the north
536 part of the domain is similarly associated with a decrease of the weekly cycle there. Note
537 that the weekly cycle of tornados only becomes established sometime in June, even
538 though tornadic activity is reaching its peak well before then (See Figure 3). We believe
539 that the consistency of these patterns of occurrence of the weekly cycle in time and space
540 and the predictions of the hypothesis that the pollution aerosols are the cause of the
541 observed weekly cycle in severe convective storms lends additional credence to our
542 hypothesis.

543 The overall statistical significance of the weekly cycles of tornado and hail activity
544 for the 15-year period 1995–2009 is quite high (see caption to Figure 4). We can also
545 examine the weekly cycle for individual summers based on sinusoidal fits to the data for
546 each summer alone, though the results are noisy given that there are only 13 weeks in a
547 summer. The results of such an analysis were displayed in earlier papers as ``clock plots''
548 for rainfall [*Bell et al*., 2008] and for lightning [*Bell et al*., 2009a]: the phase and
549 amplitude of sinusoidal fits were used to plot a point on a clock dial running from
550 Saturday to Friday and with the distance of the plot point from the center of the plot
551 proportional to the ``signal-to-noise ratio'' of the amplitude. The ``noise'' σ_7 is
552 determined from the variance of weekly fits to the data. The signal to noise ratio r_7/σ_7 is
553 given (See Eq. 4) by $[-\log(p)]^{1/2}$, where p is the significance level of the amplitude r_7, i.e.,
554 the probability that an amplitude this large could have occurred by chance, due to small-
555 sample effects, when there is in fact no weekly cycle present.
556 Despite the small number of samples in each summer of data, it was found [*Bell et*
557 *al*., 2009a] that the phases of the weekly cycles in lightning activity for summers between
558 1998 and 2009 fell year after year in the non-weekend sectors of the clock plot. This
559 strongly suggests that the weekly cycle in the data has a period of *exactly* 7 days and is
560 not an atmospheric wave with a period “in the neighborhood” of 7 days. Because tornado
561 and hail events are not nearly as numerous as lightning events, and the tornado/hail
562 observational coverage not nearly as dense, we would expect the year-by-year clock plots
563 of hail and tornado weekly cycles to be noisier than for lightning. The clock plots for hail
564 and tornados are shown in Figure 8. They cover the years 1995–2009. In order to
565 maximize the weekly cycle signal, only data from the afternoons (1200–2400 local solar

566 time), when convective instability is highest, are used in these plots. Though the phases
567 do not avoid the weekend sectors as completely as the lightning weekly-cycle phases did,
568 there is still a clear tendency for the weekly cycles of hailstorms and tornados to peak in
569 the middle of the week. When the phase falls on weekends, the signal-to-noise ratio is
570 quite low, implying that the statistical uncertainty in the determination of the phase is
571 large. Note that the hail data contain about 7 times as many events as the tornado data
572 and therefore have more stable statistics, and the phases are more consistent in avoiding
573 the weekend sectors (Figure 8a).
574
575 4.2. Results for tornados west of 100W
576 The average July dew point temperatures are smaller than 10°C at most of the area to
577 the west of 100W (see Figure 1a). Therefore we do not expect to find evidence there of
578 weekly storm invigoration. Even though there is a pronounced weekly cycle in aerosols
579 measured by ground-based EPA stations west of 100W (Figure 9), no significant weekly
580 cycle is apparent to the west of 100W (Figure 10).
581
582 **5. Discussion**
583
584 The results are in agreement with our previous reports of similar weekly cycles in the
585 rainfall [*Bell et al*., 2008] and lightning [*Bell et al*., 2009a] over the USA. The cycle was
586 ascribed there to aerosols invigorating deep convective clouds in a warm, moist
587 atmosphere. It is therefore not too surprising to find that the invigorated clouds also
588 produce more hail and tornados.
589 We show in Figure 8 that the hail and tornado data are consistent with earlier results
590 for rain and lightning in the SE U.S. in another respect: when the phase ϕ_7 and signal

591 strength r_7 for each summer of data for the years 1995–2009 are displayed on a "clock
592 plot", there is a clear tendency for the phases to avoid the weekend period, despite the
593 fact that there are only 13 weeks of data in a single summer and estimates of the weekly
594 cycle are quite noisy. It is not surprising that the avoidance is not as clear as it was for
595 the lightning data [*Bell et al*., 2009a], since lightning occurs far more frequently than
596 hailstorms and tornados and the effective sample size for lightning is far larger.
597 It is conceivable that the storm data could be affected by a weekly bias in the
598 observations of storms. However, it is shown in Figures 10a and 10b that no sign of a
599 statistically significant weekly cycle in tornado or hail occurrence is visible in the data
600 west of 100W. If there is a weekly-varying bias in storm reports it would have to be
601 present in the eastern half of the U.S. and absent in the western half to explain our results.
602 Furthermore, the weekly cycle from March to May over the eastern USA (see Figure 7),
603 is not statistically significant, and no longer points to a mid-week maximum. If anything,
604 it is pointing more towards the weekend, but without any statistical significance. This is
605 consistent with the diminution of the convective invigoration effect in cool base clouds,
606 as hypothesized by *Rosenfeld et al*. [2008]. The lack of a clear weekly cycle in the spring
607 along with its existence in the summer, plus the clear correspondence of the weekly cycle
608 that we see in the summer storm data with the cycles observed in other variables with no
609 possible weekly-varying observational bias such as lightning, cloud top heights and rain
610 intensities, suggest that the weekly cycle in storms is a real one and not an artifact of the
611 data collection methods.
612 The weekly cycle that we see is firmly pegged to the work week. It is not plausible
613 that it is a reflection of a quasi-periodic 7-day cycle in atmospheric dynamics, whose

614 phase would surely wander from year to year — something we do not see in any of the
615 clock plots. *Kim et al*. [2010] recently raised the possibility that the weekly cycle can
616 occur due to natural random variability [*Kim et al*., 2010]. This might be the case for a
617 weekly cycle that is found in general upper tropospheric synoptic features that have no
618 clear hypothesis to the way that they might be linked to anthropogenic effects [*Stinov*,
619 2010]. Weekly cycle in the instability or low level temperature being larger at the week
620 days can potentially explain greater the activity of severe convective storms at that time.
621 However, this is not likely to be the case here, based on the lack of evidence of a weekly
622 cycle in the 850 hPa temperatures and in other synoptic properties that correlate with
623 lightning activity that was presented in the supporting online materials of *Bell et al*.
624 [2009a].

625 An alternative explanation that might be considered is that the radiative effects of the
626 aerosols absorbing and reflecting the solar radiation change the atmospheric stability. If
627 anything, greater aerosol optical depth during mid-week days would reduce the surface
628 heating and suppress convection, as was shown by Koren et al. (2004 and 2008) and by
629 Rosenfeld et al. (2008).

630 Previous reports of a weekly cycle of hail in Southern France [*Dessens et al*., 2001]
631 did not show a change in hail frequency, but showed a larger kinetic energy of the
632 hailstones on weekends. It was postulated that ice forming nuclei (IFN) emitted during
633 the weekend from the local industry was creating larger number of ice hydrometeors and
634 therefore decreasing the hailstone sizes due to greater competition on the available
635 supercooled water. There is no information whether IFN have a weekly cycle in the
636 eastern USA.

637 This study has shown a clear correspondence between the weekly cycle of
638 anthropogenic aerosols and the occurrences of severe convective storms, which is highly
639 unlikely to be a result of natural variability. The observed associations cannot serve as
640 proof for causality. However, the results are consistent with the hypothesis that air
641 pollution aerosols invigorate deep convective clouds in moist and unstable atmosphere,
642 and the possibility that they can even induce the storms to produce large hail and
643 tornados. This is also consistent with the hypothesis that the severe storms are better
644 organized and violent because aerosols increase the hydrometeor size, decreasing their
645 evaporation and so weakening the negative buoyancy of the downdrafts, thereby
646 preventing the gust front from outrunning and undercutting the updraft in the feeder
647 clouds. . Anthropogenic emissions have caused large enhancements of aerosol loads
648 even over the remote continents, with typical enhancements of 50–300% over remote
649 regions of Asia, North America, and South America (Wilson et al., 2001; Chin et al.,
650 2004; Park et al., 2006; Stier et al., 2006). Regarding this increase, it is worth pointing
651 out that if a roughly 10% weekly variation in pollution levels is resulting in a similar
652 change in severe storm activity, then the "background" aerosol level, which is elevated
653 with respect to the pre-industrial level even during weekends, is also likely to be
654 changing the storm frequency that we experience today.
655
656 **Acknowledgements**
657 We thank Greg Carbin (NOAA/NWS) for his help in understanding the severe-
658 storms dataset. We also thank Earle Williams for many helpful comments on the
659 manuscript. Research by DR is an outcome of the European Community—New and

660 Emerging Science and Technologies (contract 12444 (NEST)–ANTISTORM). Research
661 by TLB was supported by the Science Mission Directorate of the National Aeronautics
662 and Space Administration as part of the Precipitation Measurement Mission program
663 under Ramesh Kakar.

664

665

666 **References**
667

668 Andreae, M. O., D. Rosenfeld, P. Artaxo, A. A. Costa, G. P. Frank, K. M. Longo, and M.
669 A. F. Silva-Dias (2004), Smoking rain clouds over the Amazon. *Science*, **303**, 1337-
670 1342.

671 Altaratz, O., I. Koren, T. Reisin, A. Kostinski, G. Feingold, Z. Levin, and Y. Yin (2008),
672 Aerosols' influence on the interplay between condensation, evaporation and rain in
673 warm cumulus cloud. Atmos. Chem. Phys., 8, 15–24.

674 Bell, T. L., and D. Rosenfeld (2008), Comment on "Weekly precipitation cycles? Lack
675 of evidence from United States surface stations" by D. M. Schultz et al. *Geophys.*
676 *Res. Lett., 35,* L09803, doi :10.1029/2007GL033046.

677 Bell, T. L., D. Rosenfeld, K.-M. Kim, J.-M. Yoo, M.-I. Lee, and M. Hahnenberger
678 (2008), Midweek increase in U.S. summer rain and storm heights suggests air
679 pollution invigorates rainstorms, *J. Geophys. Res.*, 113, D02209,
680 doi:10.1029/2007JD008623.

681 Bell, T. L., D. Rosenfeld, and K.-M. Kim (2009a), Weekly cycle of lightning: Evidence
682 of storm invigoration by pollution. Geophys. Res. Lett., 36, L23805,
683 doi:10.1029/2009GL040915.

684 Bell, T. L., J.-M. Yoo, and M.-I. Lee (2009b), Note on the weekly cycle of storm heights
685 over the southeast United States, *J. Geophys. Res.*, *114*, D15201,
686 10.1029/2009JD012041.

687 Brooks, H. E., C. A. Doswell, and M. P. Kay (2003), Climatological estimates of local
688 daily tornado probability for the United States, *Weather Forecast.*, *18*(4), 626–640.

689 Chin, M., et al., 2004. Aerosol distribution in the Northern Hemisphere during ACE-
690 Asia: results from global model, satellite observations, and sun photometer
691 measurements. J. Geophys. Res. 109 (D23), D23S90. doi:10.1029/2004JD004829.

692 Dessens, J., R. Fraile, V. Pont, and J. L. Sanchez (2001), Day-of-the-week variability of
693 hail in southwestern France, *Atmos. Res., 59*, 63–76.

694 Doswell, C. A., and D. W. Burgess (1988), On some issues of United States tornado
695 climatology, *Mon. Weather Rev.*, *116*(2), 495–501.

696 EF: http://www.spc.noaa.gov/efscale/.

697 Fan, J., T. Yuan, J. M. Comstock, S. Ghan, A. Khain, L. R. Leung, Z. Li, V. J. Martins,
698 and M. Ovchinnikov (2009), Dominant role by vertical wind shear in regulating
699 aerosol effects on deep convective clouds, *J. Geophys. Res., 114*, D22206,
700 doi:10.1029/2009JD012352.

701 Fan, J., R. Zhang, G. Li, and W.-K. Tao (2007), Effects of aerosols and relative humidity
702 on cumulus clouds. J. Geophys. Res. 112(D14): D14204.

703 Foote, G. B. (1984), A study of hail growth utilizing observed storm conditions, *J. Clim.*
704 *Appl. Meteorol., 23*, 84–101.

705 Fraser, D. A. S. (1958), *Statistics, An Introduction*, Wiley, New York, 398 pp.

706 Gunn, R. and B. B. Phillips (1957), An experimental investigation on the effect of air
707 pollution on the initiation of rain. *J. Meteorol. 14*, 272.

708 Hasselmann, K. (1979): On the signal-to-noise problem in atmospheric response studies.
709 *Meteorology Over the Tropical Oceans*, D. B. Shaw, Ed., Roy. Meteorol. Soc., 251–
710 259.

711 Khain, A. and A. Pokrovsky (2004), Simulation of effects of atmospheric aerosols on
712 deep turbulent convective clouds using a spectral microphysics mixed-phase
713 cumulus cloud model. Part II: Sensitivity study, *J. Atmos.Sci., 24*, 2983–3001.

714 Khain, A., D. Rosenfeld, and A. Pokrovsky, (2005), Aerosol impact on the dynamics and
715 microphysics of deep convective clouds, *Q. J. Roy. Meteor. Soc., 131*, 2639–2663.

716 Khain, A., N. BenMoshe, and A. Pokrovsky (2008), Factors determining the impact of
717 aerosols on surface precipitation from clouds: Attempt of classification, *J. Atmos.*
718 *Sci., 65*, 1721–1748.

719 Khain, A., L. R. Leung, B. Lynn, and S. Ghan (2009), Effects of aerosols on the
720 dynamics and microphysics of squall lines simulated by spectral bin and bulk
721 parameterization schemes, *J. Geophy. Res., 114*, D22203,
722 doi:10.1029/2009JD011902.

723 Khain, A. and B. Lynn (2009), Simulation of a supercell storm in clean and dirty
724 atmosphere using weather research and forecast model with spectral bin
725 microphysics, *J. Geophy. Res., 114*, D19209, doi:10.1029/2009JD011827.

726 Khain, A., D. Rosenfeld, A. Pokrovsky, U. Blahak and A. Ryzhkov (2011), The role of
727 CCN in precipitation and hail in a mid-latitude storm as seen in simulations using a
728 spectral (bin) microphysics model in a 2D dynamic frame. *Atmos. Res. 99*, 129-146.

729 Kim, K.-Y., R. J. Park, K.-R. Kim, and H. Na (2010), Weekend effect: Anthropogenic or
730 natural? *Geophys. Res. Lett.*, *37*, L09808, 10.1029/2010GL043233.

731 Koren, I., Y. J. Kaufman, D. Rosenfeld, L. A. Remer, Y. Rudich (2005), Aerosol
732 invigoration and restructuring of Atlantic convective clouds. *Geophys. Res. Lett., 32*,
733 L14828, doi:10.1029/2005GL023187.

734 Koren, I., Y.J. Kaufman, L.A. Remer and J.V. Martins, 2004: Measurement of the effect
735 of Amazon smoke on inhibition of cloud formation. *Science, 303*, 1342-1345.

736 Koren, I., J. V. Martins, L.A. Remer, H. Afargan (2008), Smoke invigoration versus
737 inhibition of clouds over the Amazon. *Science*, *321*, no. 5891, 946–949.

738 Koren, I., L. A. Remer, O. Altaratz, J. V. Martins, and A. Davidi (2010), Aerosol-induced
739 changes of convective cloud anvils produce strong climate warming. *Atmos. Chem.*
740 *Phys. 10,* 5001–5010.

741 Langenberg, H. (2011), Triggered lightning. In "news and views", *Nature Geosceince, 4*,
742 140.

743 Li, G., Y. Wang, and R. Zhang (2008): Implementation of a two-moment bulk
744 microphysics scheme to the WRF model to investigate aerosol-cloud interaction. *J.*
745 *Geophys. Res., 113*, D15211, doi:10.1029/2007JD009361.

746 Lee, J.-S. (1986), Speckle suppression and analysis for synthetic aperture radar images,
747 *Opt. Engineer.*, *25*(5), 636–643.

748 Lee, S. S., L. J. Donner, and J. E. Penner (2010), Thunderstorm and stratocumulus: how
749 does their contrasting morphology affect their interactions with aerosols? *Atmos.*
750 *Chem. Phys., 10*, 6819–6837.

751 Lee, S. S., L. J. Donner, V. T. J. Phillips, and Y. Ming (2008a), Examination of aerosol
752 effects on precipitation in deep convective clouds during the 1997 ARM summer
753 experiment, *Q. J. Roy. Meteor. Soc., 134*, 1201–1220.

754 Lee, S. S., L. J. Donner, V. T. J. Phillips, and Y. Ming (2008b), The dependence of
755 aerosol effects on clouds and precipitation on cloud system organization, shear and
756 stability, *J. Geophys. Res., 113*, D16202, doi:10.1029/2007JD009224.

757 Lerach, D. G., B. J. Gaudet, and W. R. Cotton (2008), Idealized simulations of aerosol
758 influences on tornadogenesis, *Geophys. Res. Lett., 35*, L23806,
759 doi:10.1029/2008GL035617.

760 Ludlam, F. H. (1963), Severe local storms: A review, in *Severe Local Storms, Meteorol.*
761 *Monogr., 27*, 1–30, Am. Meteorol. Soc., Boston, Mass.

762 Lyons, W. A., T. E. Nelson, E. R. Williams, J. A. Cramer, and T. R. Turner (1998),
763 Enhanced positive cloud-to-ground lightning in thunderstorms ingesting smoke from
764 fires, *Science, 282*(5386), 77–80, doi:10.1126/science.282.5386.77.

765 Markowski, P. M., J. M. Straka, and E. N. Rasmussen (2002), Direct surface
766 thermodynamic observations within the rear-flank downdrafts of nontornadic and
767 tornadic supercells, *Mon. Weather Rev., 130*, 1692–1721.

768 Markowski, P. M., J. M. Straka, and E. N. Rasmussen (2003), Tornadogenesis resulting
769 from the transport of circulation by a downdraft: Idealized numerical simulations, *J.*
770 *Atmos. Sci., 60*, 795– 823.

771 Molinié, J., C. Pontikis (1995), A climatological study of tropical thunderstorm clouds
772 and lightning frequencies on the French Guyana coast, *Geophys. Res. Lett. 22*, 1085–
773 1088.

774 Ntelekos, A. A., J. A. Smith, L. Donner, J. D. Fast, W. I. Gustafson Jr., E. G. Chapman,
775 and W. F. Krajewski (2009), The effects of aerosols on intense convective
776 precipitation in the northeastern United States. *Quart. J. Roy. Meteor. Soc., 135*,
777 1367–1391.
778 NOAA National Weather Service (2007), Storm Data Preparation,
779 http://www.weather.gov/directives/sym/pd01016005curr.pdf.
780 Park, R.J., Jacob, D.J., Kumar, N., Yantosca, R.M., 2006. Regional visibility statistics in
781 the United States: natural and transboundary pollution influences, and implications
782 for the Regional Haze Rule. *Atmos. Environ. 40* (28), 5405–5423.
783 Ray, P. S., P. Bieringer, X. F. Niu, and B. Whissel (2003), An improved estimate of
784 tornado occurrence in the Central Plains of the United States, *Mon. Weather Rev.*,
785 *131*(5), 1026–1031.
786 Rosenfeld, D. and C. W. Ulbrich (2003), Cloud microphysical properties, processes, and
787 rainfall estimation opportunities. Chapter 10 of " Radar and Atmospheric Science: A
788 Collection of Essays in Honor of David Atlas". Edited by Roger M. Wakimoto and
789 Ramesh Srivastava. *Meteorological Monographs* **52**, 237-258, AMS.
790 Rosenfeld, D., U. Lohmann, G.B. Raga, C.D. O'Dowd, M. Kulmala, S. Fuzzi, A.
791 Reissell, M.O. Andreae (2008), Flood or Drought: How Do Aerosols Affect
792 Precipitation? *Science, 321*, 1309-1313.
793 Schaefer, J. T., and R. Edwards (1999), The SPC Tornado/Severe Thunderstorm
794 Database, in *Preprints of the 11th Conf. Appl. Climatology, Dallas, TX*.

795 Snook, N., M. Xue (2008), Effects of microphysical drop size distribution on
796 tornadogenesis in supercell thunderstorms. *Geophys. Res. Lett., 35*, L24803,
797 doi:10.1029/2008GL035866.

798 SPC Data (2010): http://www.spc.noaa.gov/wcm/index.html#data

799 Stier, P., Feichter, J., Roeckner, E., Kloster, S., Esch, M., 2006. The evolution of the
800 global aerosol system in a transient climate simulation from 1860 to 2100. *Atmos.*
801 *Chem. Phys., 6*, 3059–3076.

802 Stinov, S. A. (2010), Weekly cycle of meteorological parameters over Moscow region,
803 *Doklady Earth Sciences, 431*, 507-513. DOI 10.1134/S1028334X10040203.

804 Storer, R. L., S. C. van den Heever, and G. L. Stephens (2010), Modeling aerosol impacts
805 on convective storms in different environments. *J. Atmos. Sci., 67*, 3904–3915. doi:
806 10.1175/2010JAS3363.1

807 Tao, W.-K., X. Li, A. Khain, T. Matsui, S. Lang, and J. Simpson (2007), The role of
808 atmospheric aerosol concentration on deep convective precipitation: cloud-resolving
809 model simulations, *J. Geophys. Res., 112*, D24S18, doi:10.1029/2007JD008728.

810 van den Heever, S. C., and W. R. Cotton (2004), The impact of hail size on simulated
811 supercell storms, *J. Atmos. Sci., 61*, 1596–1609.

812 van den Heever, S. C., G. G. Carrió, W. R. Cotton, P. J. DeMott, and A. J. Prenni (2006),
813 Impacts of nucleating aerosol on Florida storms. Part I: Mesoscale simulations. *J.*
814 *Atmos. Sci., 63*, 1752–1775.

815 van den Heever, S. C., and W. R. Cotton (2007), Urban aerosol impacts on downwind
816 convective storms. *J. Appl. Meteor. Climatol., 46*, 828–850

817 Wang, C. (2005), A modeling study of the response of tropical deep convection to the
818 increase of cloud condensation nuclei concentration: 1. Dynamics and microphysics,
819 *J. Geophys. Res., 110*, D21211, doi:10.1029/2004JD005720.
820 Wang, J., S. C. van den Heever, J. S. Reid (2009), A conceptual model for the link
821 between Central American biomass burning aerosols and severe weather over the
822 south central United States. *Environ. Res. Lett.* 4, 015003, doi: 10.1088/1748-
823 9326/4/1/015003.
824 Wilks, D. S. (2006), On "field significance" and the false discovery rate, *J. Appl.*
825 *Meteorol. Clim.*, *45*, 1181–1189.
826 Williams, E. R. (2005), Lightning and climate: A review, *Atmos. Res., 76*(1–4), 272–287,
827 doi:10.1016/j.atmosres.2004.11.014.
828 Williams, E., D. Rosenfeld, M. Madden et al. (2002), Contrasting convective regimes
829 over the Amazon: Implications for cloud electrification. *J. Geophys. Res., 107*
830 (D20), 8082, doi:10.1029/2001JD000380.
831 Williams, E., and S. Stanfill (2002), The physical origin of the land-ocean contrast in
832 lightning activity, *C. R. Phys., 3*(10), 1277–1292, doi:10.1016/S1631-
833 0705(02)01407-X.
834 Williams, E., V. Mushtak, D. Rosenfeld, S. Goodman and D. Boccippio, 2005:
835 Thermodynamic conditions favorable to superlative thunderstorm updraft, mixed
836 phase microphysics and lightning flash rate. *Atmospheric Research*, **76**, 288-306.
837 Wilson, J., Cuvelier, C., Raes, F., 2001. A modeling study of global mixed aerosol fields.
838 *J. Geophys. Res. 106* (D24), 34,081–34,108.

839 Yuan, T., L. A. Remer, K. E. Pickering, and H. Yu (2011), Observational evidence of
840 aerosol enhancement of lightning activity and convective invigoration. *Geophys*.
841 *Res*. *Lett*., *38*, L04701, doi:10.1029/2010GL046052.
842 Zhang, R., G. Li, J. Fan, D. L. Wu, and M. J. Molina (2007), Intensification of Pacific
843 storm track linked to Asian pollution, 2007. *PNAS 108* (13) 5295-5299;
844 doi:10.1073/pnas.0700618104.
845
846
847
848

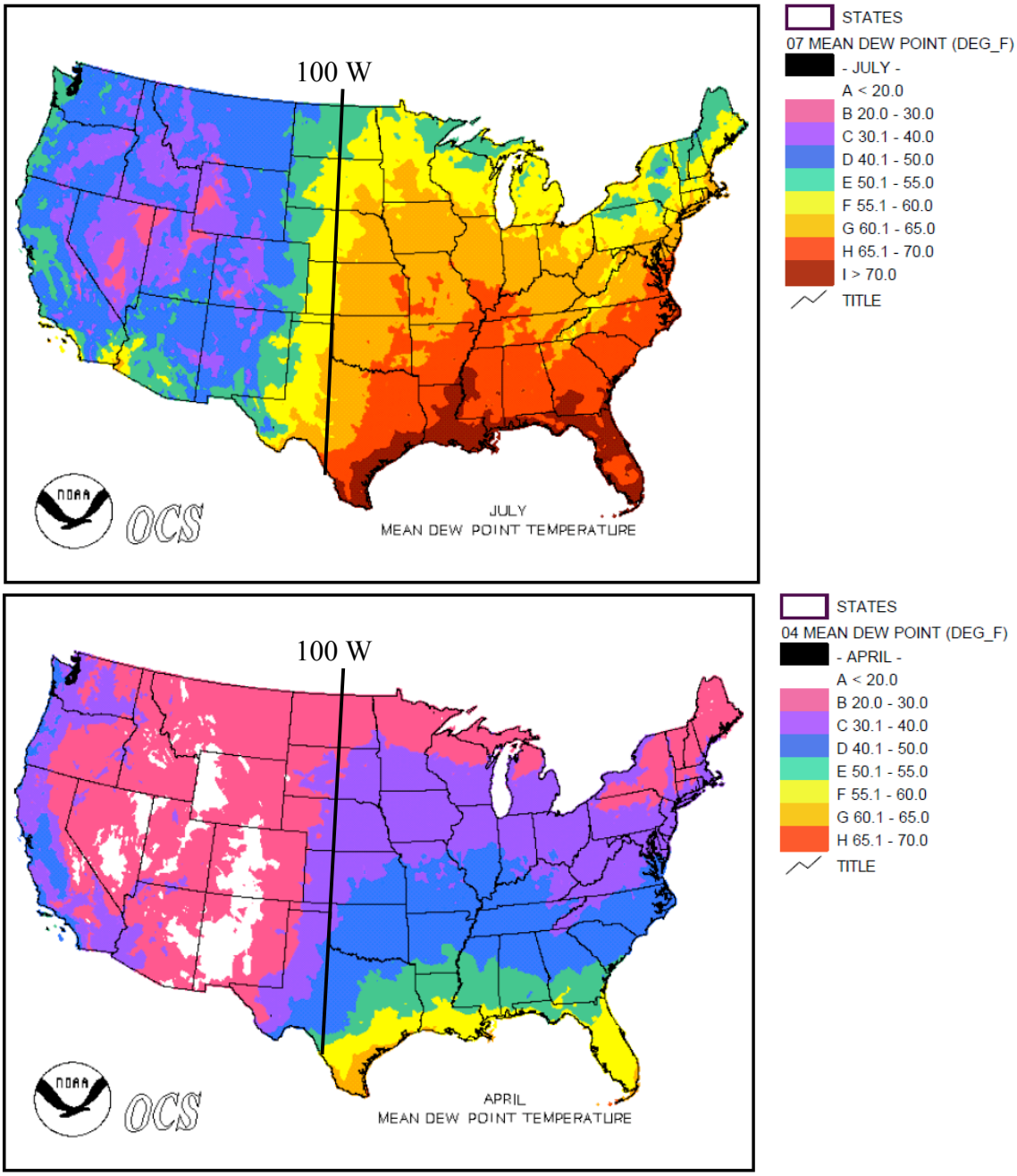

Figure 1: Mean dew point temperature for July (top) and April (bottom). From NOAA Climatic Data Center.

855 **FIGURES**

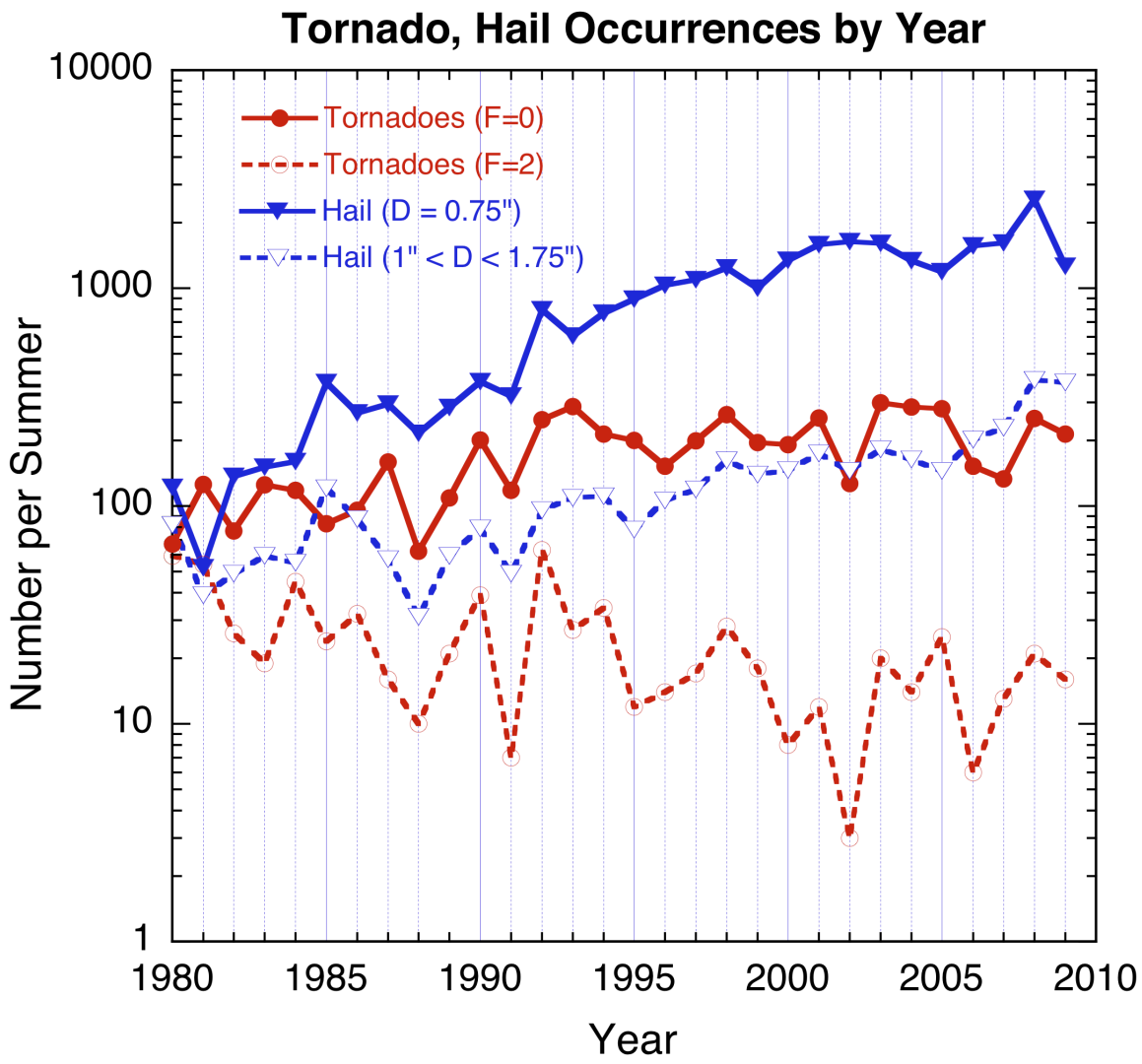

856

857 Figure 2. Number of tornado and hailstorm events each summer (Jun–Aug) for 1980–
858 2009. Graphs are shown for tornados classified as F0 and as F2 in strength, and for
859 hailstorms with reported hail diameters of 0.75 inches, and between 1 and 1.75 inches
860 (exclusive). (Because hail diameters are generally given in 0.25-inch increments, this bin
861 includes mostly hail diameters of 1.25 and 1.5 inches.)
862

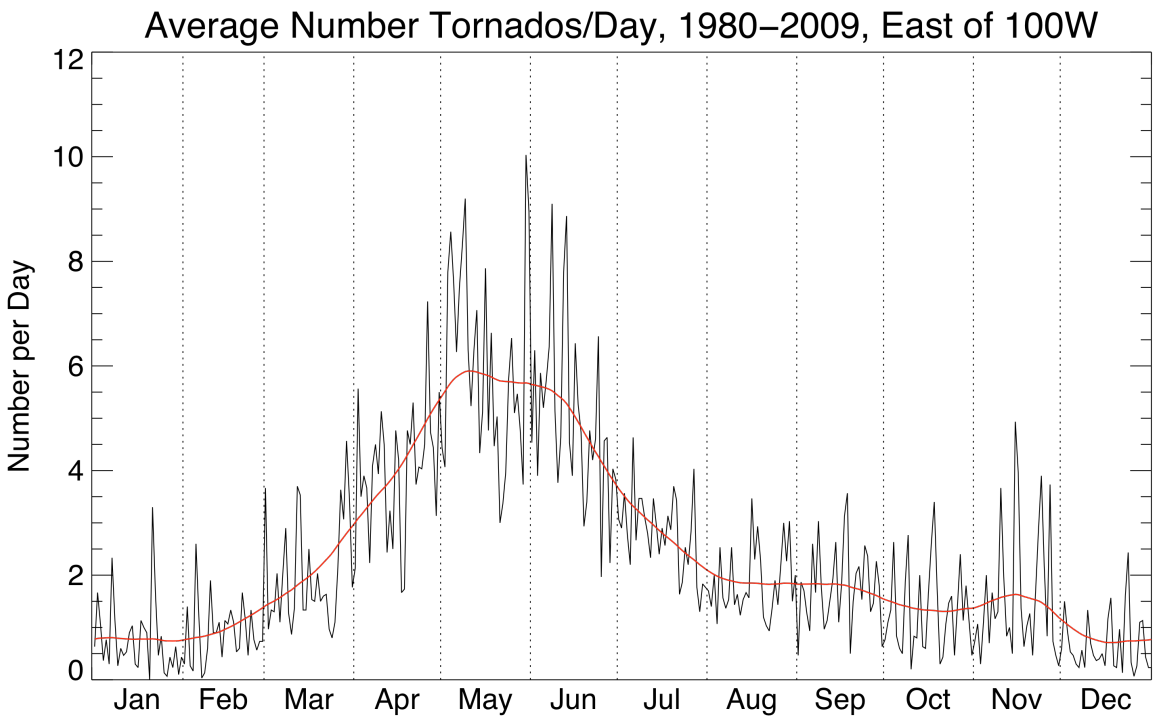

Figure 3: Average number of tornados per day (jagged black curve), all strengths, for years 1980–2009. Smooth red curve shows fit to data using Lee filter, as described in the text, and was used by us as the expected tornado count for days of the year. It is denoted by *f(j)* in the text.

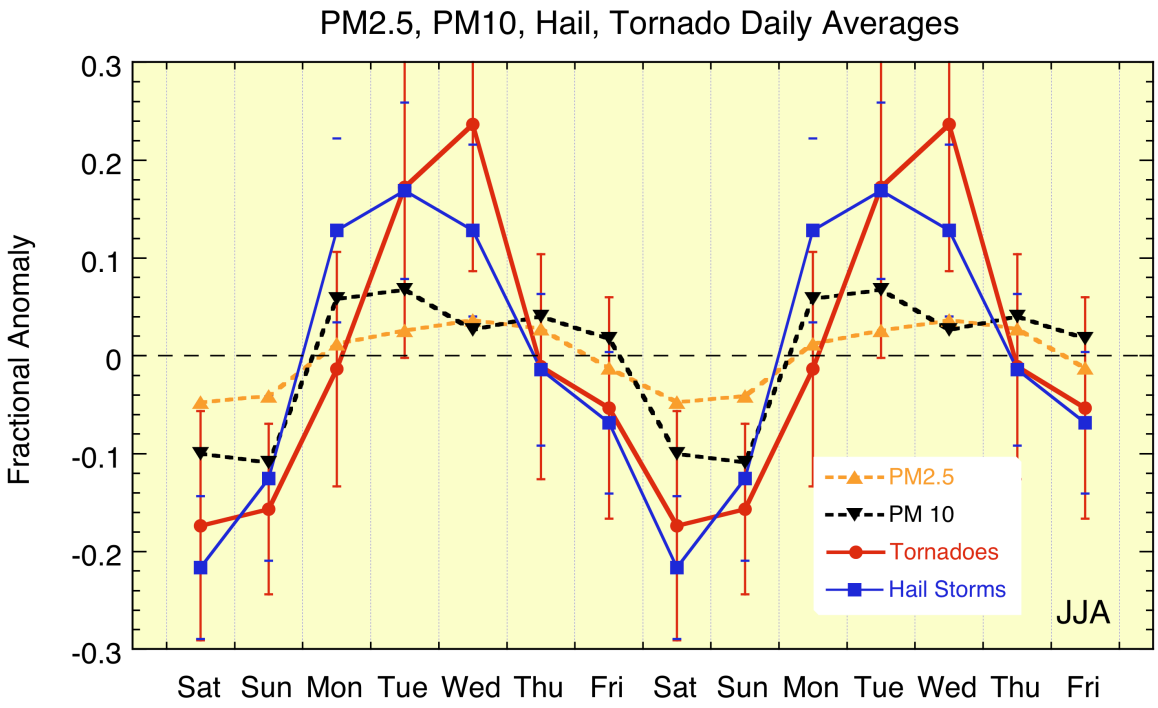

Figure 4: Weekly cycle of the aerosols (PM2.5 and PM10), as measured by the EPA over the USA during JJA of 1998-2005 east of 100W within the continental USA, along with the associated weekly cycle of the SPC-reported hailstorms and tornados over the same area averaged over JJA for 1995–2009. The value shown for each day of the week, for tornado and hail, is a straightforward average of the recorded occurrences for that day of the week, expressed as a fractional anomaly (the deviation of the average from the 7-day mean divided by the mean). The values shown for PM data are averages over all sites of the fractional anomalies computed at each EPA site for which there are data. The significance levels p for the weekly cycle of tornados are $p = 0.011$ (F-test) and $p = 0.033$ (bootstrap test). The significance levels for the hail data are $p = 0.00013$ (F-test) and $p = 0.0008$ (bootstrap tests with 10^4 simulated datasets). The error bars for the hail are shown only as short horizontal blue lines. The plots repeat the first 7 days in order to better display the nature of the weekly variations.

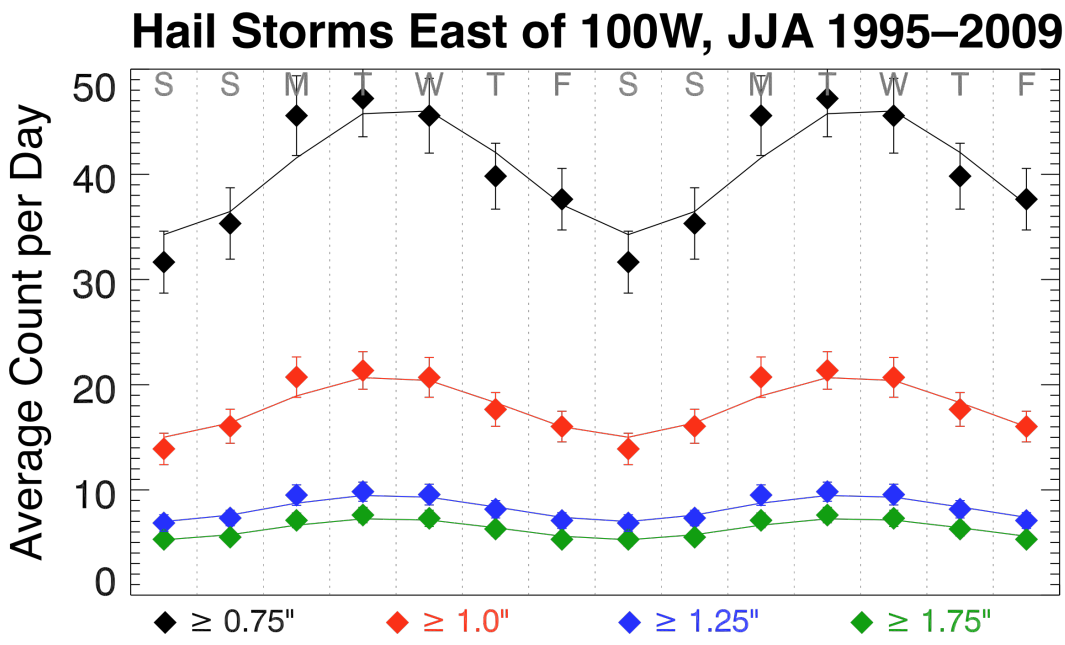

Figure 5a. Daily averages for hail occurrences of various strengths (hail diameters) are shown, using data for hailstorms east of 100W within the continental USA for June–August, 1995–2009. Smooth curves are sinusoidal fits to data.

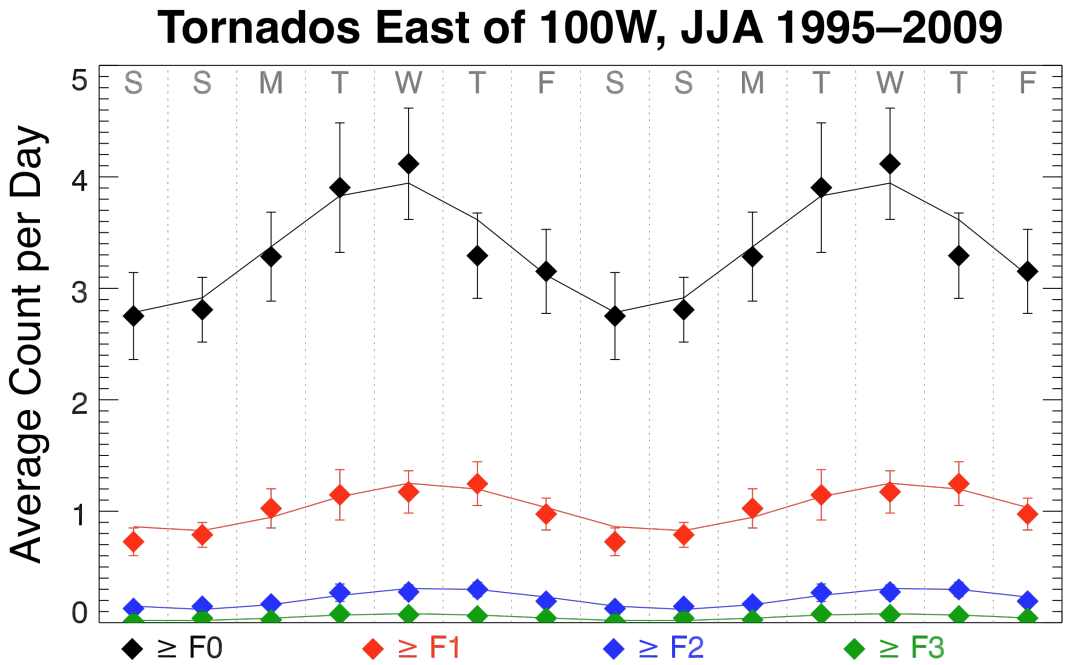

Figure. 5b. Daily averages for tornado occurrences of various strengths (F values) are shown, using data for tornados east of 100W within the continental USA for June–August, 1995–2009. Smooth curves are sinusoidal fits to data.

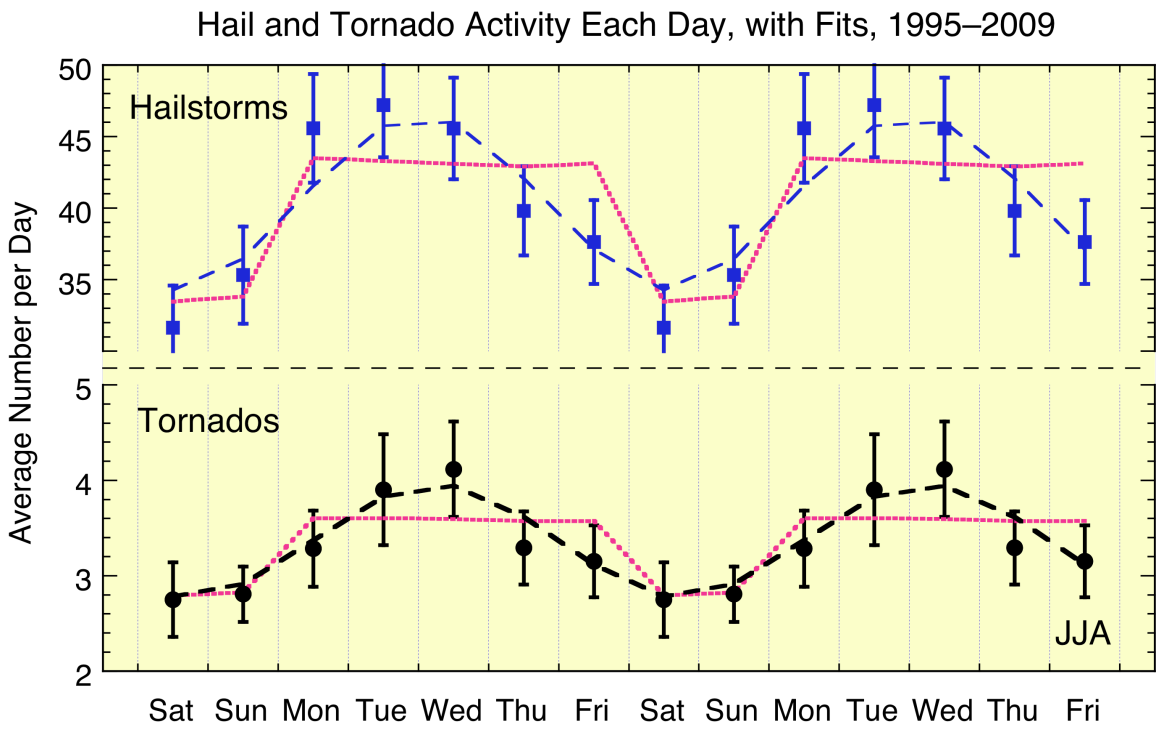

Figure. 6. Day-of-the-week averages for tornado and hailstorm occurrences of all strengths, with step-function (dotted curve) and sinusoidal (dashed curve) fits superimposed. Error bars are estimated standard errors of averages (i.e., "1-sigma errors"). All events east of 100W within the continental USA are counted, using June–August, 1995–2009 data. Significance levels for fits are given in the text.

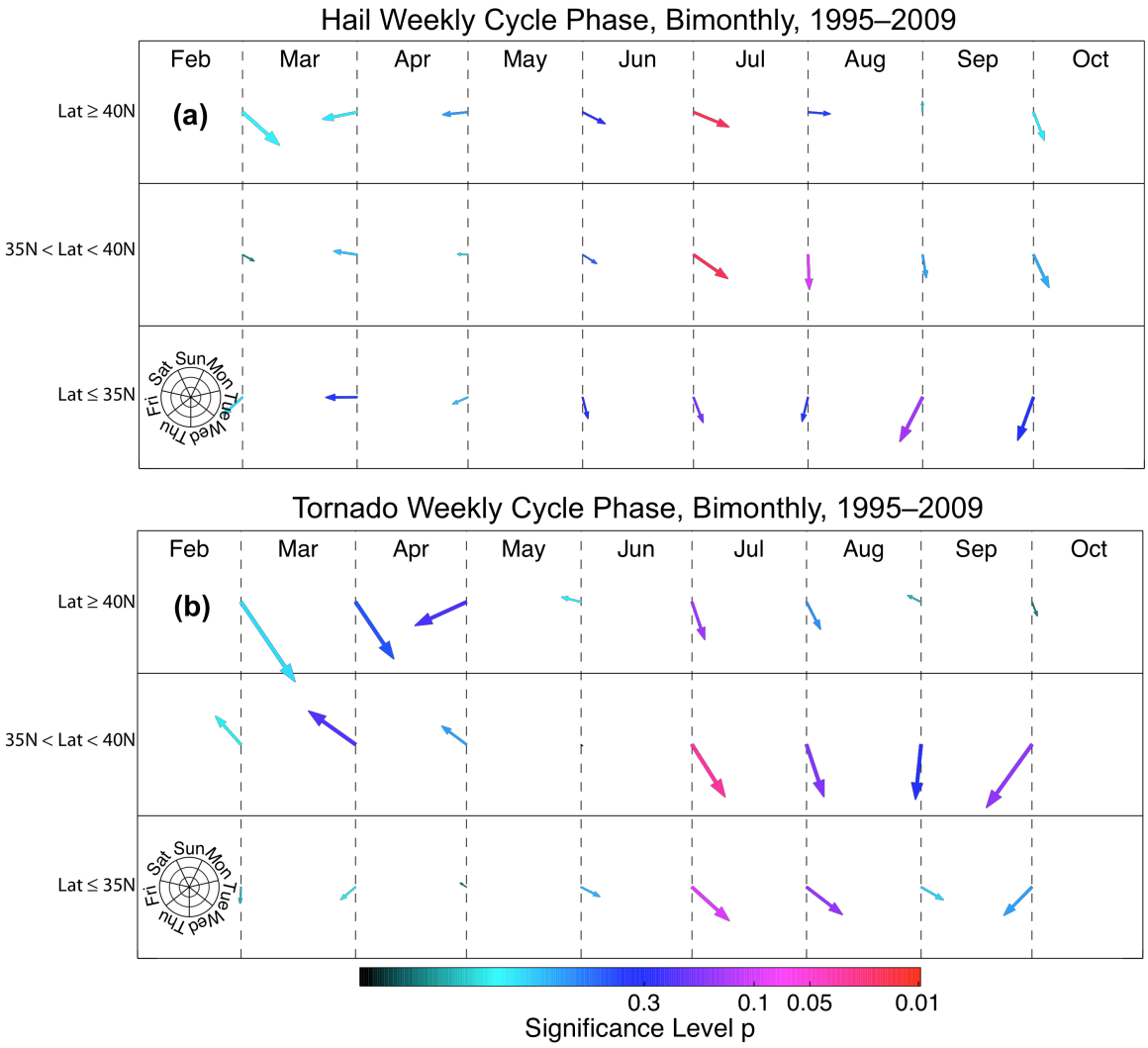

Figure 7: The dependence of the phase of the weekly cycle in hail (a) and tornadic (b) storms on the time of year and geographical latitude (for all storms east of 100W within the continental USA). Each arrow represents averages of the two months to either side of its location. The latitudes contributing to each row of statistics are shown to the left of the figure. The arrow points to the day of the week when the sinusoidal fit is a maximum, and the length indicates the weekly amplitude as a fraction of the bimonthly mean, according to the key at the bottom left of the figures. The radius of the outermost

913 circle in the key represents a fractional anomaly of 0.15. The arrows are colored
914 according to their significance level, with the color bar below indicating the significance
915 level assigned to each color.
916

916

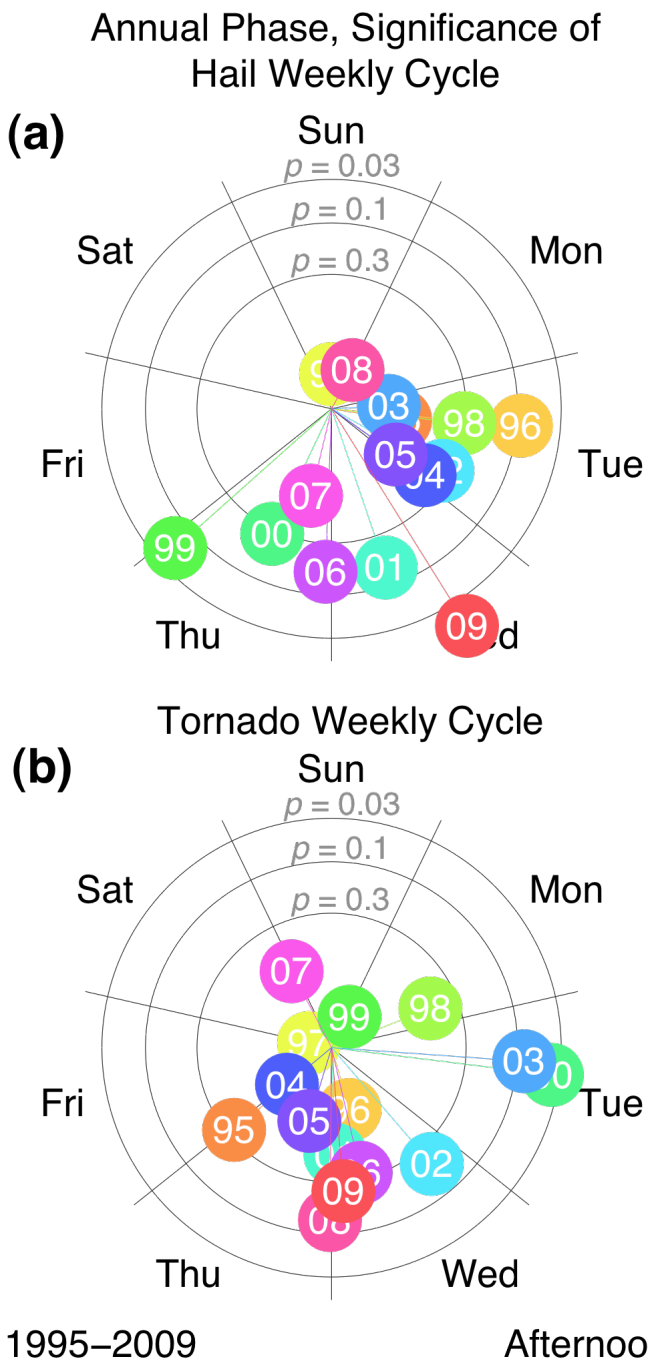

917

918 Figure 8: The phase (day of the week) and amplitude of the weekly cycle (Eq. 3) of data
919 for each summer for the years 1995–2009. The amplitude is represented by the distance
920 from the origin and is proportional to the signal-to-noise ratio of the amplitude, r_7/σ_7.
921 The last two digits of the year are shown in the colored balloons. The probability p that

the amplitude of the weekly cycle could exceed a given radius, under the null hypothesis $r_7 = 0$, is shown by the circles labeled by the corresponding value of p. (a) Hail data. (b) Tornado data.

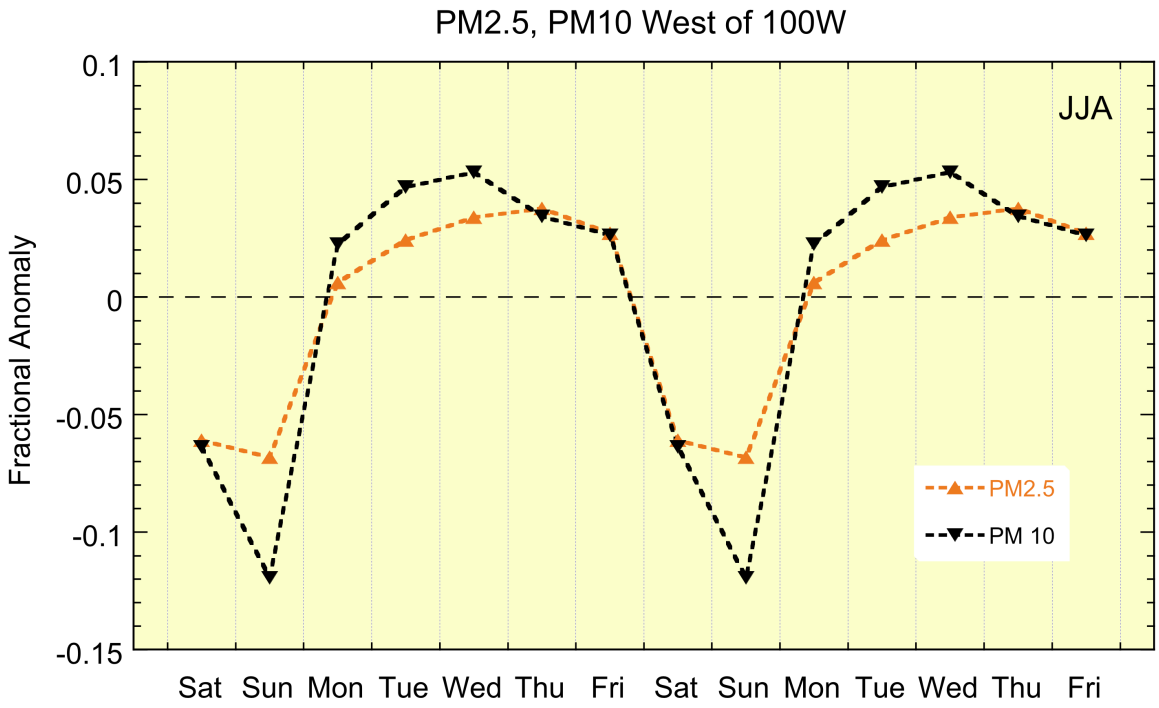

Figure 9. Weekly cycle of the aerosol concentrations (PM2.5 and PM10), as measured by the EPA over the USA during JJA of 1998–2005 to the west of 100W within the continental USA. Daily averages are expressed as fractional anomalies relative to the overall means.

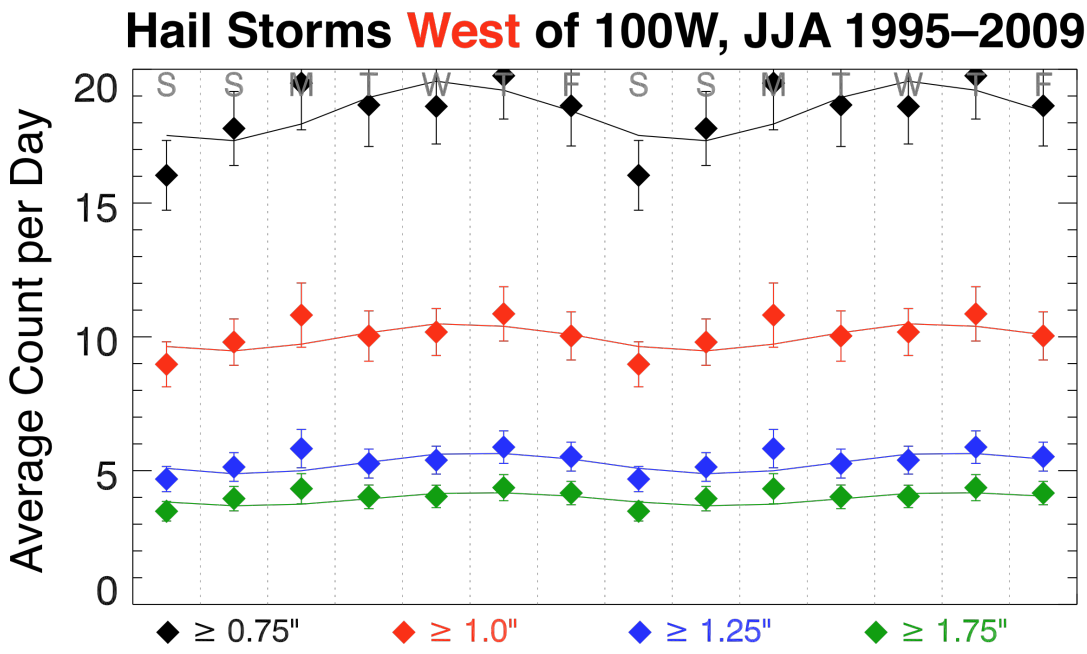

Figure 10a. Daily averages for hailstorm occurrences of various strengths (hail diameters) are shown, using data for hailstorms west of 100W within the continental USA in JJA and for 1995–2009. Smooth curves are sinusoidal fits to data. The weekly cycles are not statistically significant.

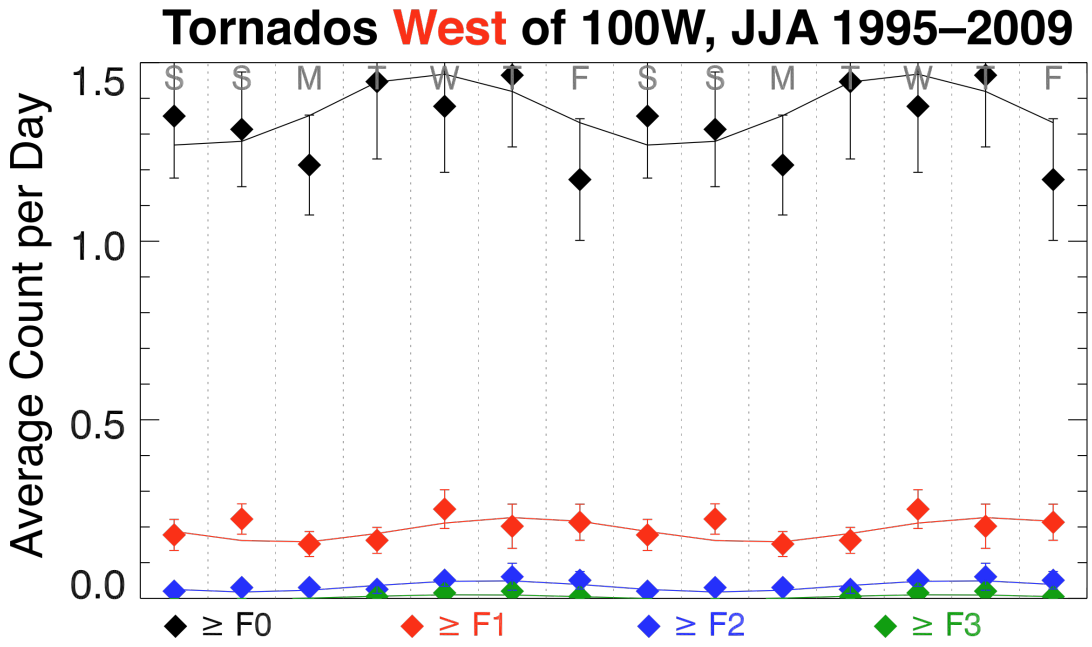

Figure 10b. Daily averages for tornado occurrences of various strengths (EF values) are shown, using data for tornados west of 100W within the continental USA in JJA and for

943 1995–2009. Smooth curves are sinusoidal fits to data. The weekly cycles are not
944 statistically significant.
945